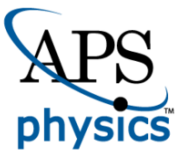

Trapping Rydberg Atoms in an Optical Lattice

S. E. Anderson, K. C. Younge, and G. Raithel

Phys. Rev. Lett. **107**, 263001 — Published 20 December 2011

DOI: 10.1103/PhysRevLett.107.263001

Trapping Rydberg atoms in an optical lattice

S. E. Anderson*, K. C. Younge, and G. Raithel
FOCUS Center, Department of Physics, University of Michigan, Ann Arbor, MI 48109

Rubidium Rydberg atoms are laser-excited and subsequently trapped in a one-dimensional optical lattice (wavelength 1064 nm). Efficient trapping is achieved by a lattice inversion immediately after laser excitation using an electro-optic technique. The trapping efficiency is probed via analysis of the trap-induced shift of the two-photon microwave transition $50S \rightarrow 51S$. The inversion technique allows us to reach a trapping efficiency of 90%. The dependence of the efficiency on the timing of the lattice inversion and on the trap laser power is studied. The dwell time of $50D_{5/2}$ Rydberg atoms in the lattice is analyzed using lattice-induced photo-ionization.

PACS numbers: 37.10.Jk, 32.30.Bv, 32.80.Ee

Rydberg-atom trapping has emerged as a tool in quantum computing [1–4] and high precision spectroscopy [5]. Small lattice-induced energy-level shifts distinguish optical Rydberg-atom traps from static-field traps [6, 7] and make them attractive for these applications. Electro- or magneto-static Rydberg traps have trap-induced shifts of the order of GHz, while shifts induced by an optical-lattice trap are in the MHz range [8] and could be reduced further by lowering atom temperature and lattice depth. Despite potential applications, efficient optical lattice traps for Rydberg atoms have not been realized until now. In this Letter, we demonstrate an optical lattice with high Rydberg-atom trapping efficiency.

The trapping of Rydberg atoms in an optical lattice arises from the ponderomotive force. In a laser field with electric-field amplitude E and angular frequency ω, the quasi-free Rydberg electron experiences an energy shift given by the free-electron ponderomotive potential, $V_\mathrm{p} = e^2E^2/(4m_\mathrm{e}\omega^2)$ [9], which is equivalent to a polarizability $\alpha_\mathrm{p} = -e^2/(m_\mathrm{e}\omega^2)$ (e is the elementary charge and m_e the electron mass). In an optical lattice, V_p is periodic in space and traps the quasi-free Rydberg electron at lattice intensity minima. The entire atom is then trapped since the Rydberg atom's ionic core is weakly bound to the Rydberg electron. Adiabatic Rydberg-atom trapping potentials have been calculated in Refs. [8, 10].

We investigate the trapping of ^{85}Rb Rydberg atoms in a one-dimensional optical lattice of wavelength $\lambda =$ 1064 nm, for which $\alpha_\mathrm{p} = -4\pi\epsilon_0 \times 545a_0^3$. For atoms in the 5S ground state, the lattice is red-detuned relative to the $5S \rightarrow 5P$ transition, resulting in a positive dynamic polarizability, $\alpha_\mathrm{5S} = 4\pi\epsilon_0 \times 711a_0^3$ [11]. Due to the different signs of α_p and α_5S, the ground-state lattice potential minima, which are located at light intensity maxima, coincide with Rydberg-state potential maxima. Ground-state atoms are initially laser-cooled into the wells of the $5S$ lattice potential. Laser excitation of these atoms produces Rydberg atoms near the maxima of the Rydberg-atom lattice potential. Previously, we have trapped a few percent of these atoms in the lattice [12]. In the present work, we develop a method to rapidly invert the lattice potential after Rydberg atom preparation. Since the inverted potential has minima near the locations of the initially prepared Rydberg atoms, highly efficient optical Rydberg-atom trapping is achieved.

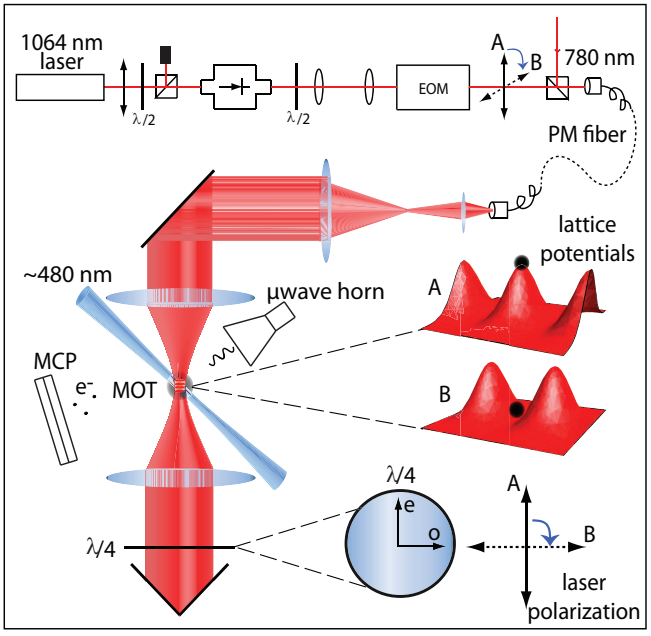

FIG. 1. (Color online.) Sketch of the experimental setup. Rydberg atoms are optically excited at potential maxima of a one-dimensional Rydberg-atom optical lattice. An electro-optic modulator (EOM) is used to switch the lattice polarization by 90° from A to B immediately after excitation, resulting in lattice inversion and efficient Rydberg atom trapping.

The experimental setup is illustrated in Fig. 1. ^{85}Rb atoms are loaded into a magneto-optical trap (MOT) with a temperature ∼200 μK. The lattice is established by focusing the 1064 nm beam into the MOT [power up to 1.2 W, full-width at half maximum of the intensity profile (FWHM) of 13 μm], retro-reflecting and refocusing it. The lattice is always on and forms wells with depth up to about 20 MHz for the ground and 10 MHz for the Rydberg state. The center-of-mass atom motion is the classical regime, and tunneling is unimportant. The focus of

the ingoing beam of the lattice is aligned by maximizing the lightshift induced in the optical Rydberg excitation. The return-beam focus is positioned by optimizing the back-coupling through the fiber shown in Fig. 1. Simulations, discussed below, yield a best-fit temperature of $\sim$100 μK for the ground-state atoms in the optical lattice, indicating that the atoms experience moderate sub-Doppler cooling when falling from the MOT into the optical lattice.

In an experimental cycle, the MOT is turned off, and excitation pulses of duration $\tau_{\rm ex} = 0.5$ μs to 2 μs are applied to prepare Rydberg atoms. The lower-transition laser (FWHM 150 μm) has a wavelength of 780 nm and is $\approx$1.2 GHz detuned from the $5P_{3/2}$ intermediate state. The upper-transition laser wavelength is $\approx$480 nm (FWHM $\sim$15 μm) and is tuned into two-photon resonance with the $5S \rightarrow 50S$ transition at lattice intensity maxima. The optical excitation beams cover about 50 lattice planes, each of which contains up to about 10 ground-state atoms. To avoid Rydberg-Rydberg interaction, for all $\tau_{\rm ex}$ the excitation pulse powers are kept sufficiently low that fewer than 2 Rydberg atoms are excited in the entire sample (*i.e.*, the single-atom excitation probability is below 1% and far from saturation). After the excitation pulse, the lattice is inverted. The Rydberg atoms then interact for 6 μs with microwave radiation that drives the $50S \rightarrow 51S$ two-photon transition. Subsequently, the Rydberg-state distribution is measured using state-selective electric field ionization [13]. The freed electrons are detected using a micro-channel plate detector. Reference [12] contains further experimental details.

The lattice inversion is accomplished with an electro-optic modulator (EOM; Fig. 1). The EOM is used as a polarization switch that splits the incident total power P into two orthogonal linear-polarization components with variable powers $P_{\rm trans}$ and $P - P_{\rm trans}$, which are then transmitted to the atoms using a polarization-maintaining (PM) fiber. The polarization directions are aligned with the axes of a quarter waveplate in the return beam of the lattice (see Fig. 1) that introduces a total differential phase shift of π between the polarization components. We characterize the lattice inversion by the parameter $\eta = P_{\rm trans}/P$, which ranges from zero (no inversion) to 1 (complete inversion). Lattice potentials for selected values of η are depicted in Fig. 2(b). For the lattice inversion to be most effective, the timescale over which the inversion occurs must be faster than the center-of-mass oscillation period of the atoms in the lattice. In our lattice, the oscillation period is $\sim$5 μs while 85% of the polarization switch occurs within 0.2 μs.

We investigate the Rydberg-atom trapping efficiency of the lattice through microwave spectroscopy of the $50S \rightarrow 51S$ transition. This method exploits the fact that the lattice-induced shift of the microwave transition depends on the atomic position in the lattice [12]. Without inversion ($\eta = 0$), the microwave spectra exhibit

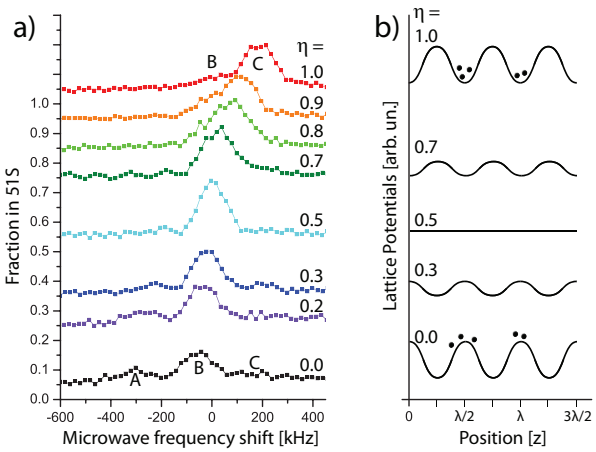

FIG. 2. (Color online.) a) Experimental microwave spectra for $P = 0.8$ W and optical pulse length $\tau_{\rm ex} = 0.5$ μs for the indicated values of $\eta = P_{\rm trans}/P$ (spectra offset for clarity). b) Lattice potentials after inversion vs position for several of the η-values used in panel (a). The fully inverted case, $\eta = 1$, leads to the strongest blue-shifted signal component, indicative of most efficient Rydberg-atom trapping.

three features, labeled A, B, and C in the lowermost spectrum in Fig. 2(a). The red-shifted feature A is associated with un-trapped atoms that spend the majority of the time near a lattice potential maximum. Feature B is due to un-trapped atoms with trajectories traversing several lattice wells. The blue-shifted feature C is largely due to atoms trapped in a single lattice well. Without lattice inversion, the C-signal is weak, and only a few percent of the Rydberg atoms are trapped. The case $\eta = 0$ is analyzed in detail in Refs. [12, 14].

In Fig. 2(a) we show microwave spectra for several values of η. As η is increased from 0 to 1, the signal shifts almost entirely into the C-component, which presents a qualitative measure for the fraction of trapped atoms. Hence, the $\eta = 1$ spectrum demonstrates that the fully inverted lattice forms a highly efficient Rydberg-atom trap. The high trapping efficiency occurs because the Rydberg atoms do not significantly move during the optical excitation pulse length ($\tau_{\rm ex} = 0.5$ μs) and the 0.2 μs lattice inversion time. Following the lattice inversion, the atoms find themselves trapped at a minimum of the Rydberg-atom trapping potential, despite the fact that they were initially excited at a maximum of that potential. Integrating the areas under the B and C-signals in the curve for $\eta = 1$ in Fig. 2(a), we obtain a first estimate of the trapping efficiency of about 80%. However, we expect this estimate to be too low because the red-detuned Fourier side peaks of the strong C-component overlap with the relatively weak B-component.

In order to obtain a more accurate estimate of the trapping efficiency, we perform simulations to model the entire microwave spectrum [12]. In the simulations, initial positions and velocities of $5S$ atom ensembles are de-

termined from a Maxwell-Boltzmann distribution in the ground-state trapping potential (temperature T). The optical excitation $5S \rightarrow 50S$ is assumed to be resonant at the lattice intensity maxima, where the $5S$ atoms collect, and we assume low saturation and an excitation bandwidth of 3 MHz (the measured width of lattice-free optical Rydberg resonance lines). The atom-lattice interaction times are randomly chosen between 6 μs and 6 μs+$\tau_{\rm ex}$, consistent with the timing used in the experiment. The classical center-of-mass Rydberg-atom trajectories follow from the trapping potential calculated for the Rydberg levels [10]. The microwave-driven quantum evolution in the internal state space $\{|50S\rangle, |51S\rangle\}$ is computed along these trajectories by integrating the time-dependent Schrödinger equation. In Fig. 3, we show theoretical spectra obtained for our experimental conditions, as well as 100 typical Rydberg-atom trajectories for the cases $\eta = 0$ and $\eta = 1$.

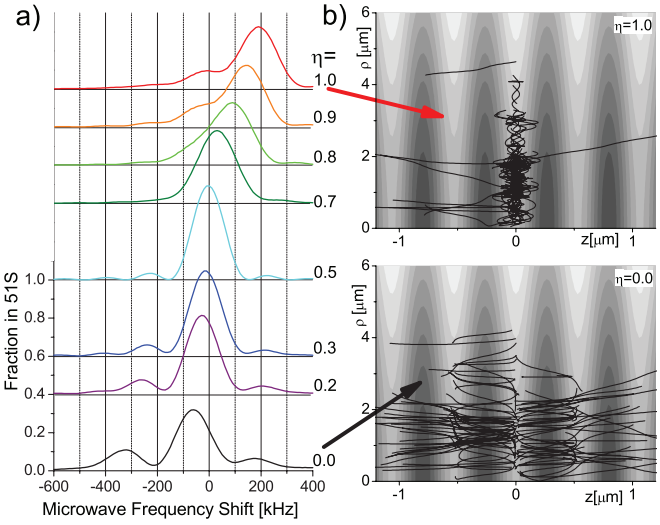

FIG. 3. (Color online.) a) Simulated microwave spectra for the indicated values of $\eta = P_{\rm trans}/P$ and the same conditions as in Fig. 2. b) Simulated atomic trajectories for the cases of no inversion (bottom) and complete inversion (top). The Rydberg-atom trapping potential is shown in the background on a scale from 3 MHz (white) to 15 MHz (dark).

Most parameters in the simulation have values known from the experiment. The Rabi frequency of the microwave transition is set to a fixed value at which the on-resonant $50S \rightarrow 51S$ transition probability is 50% when the lattice is off (as in the experiment). The measured powers of the incident and return lattice beams and the measured FWHM diameter of the incident lattice beam (13 μm) are also entered as fixed values. The only free fit parameters of the simulation are the initial atom temperature T and the FWHM diameter of the return lattice beam, $w_{\rm r}$, which could not be measured.

Excellent agreement between experimental and simulated microwave spectra is found for $w_{\rm r} = 25$ μm and

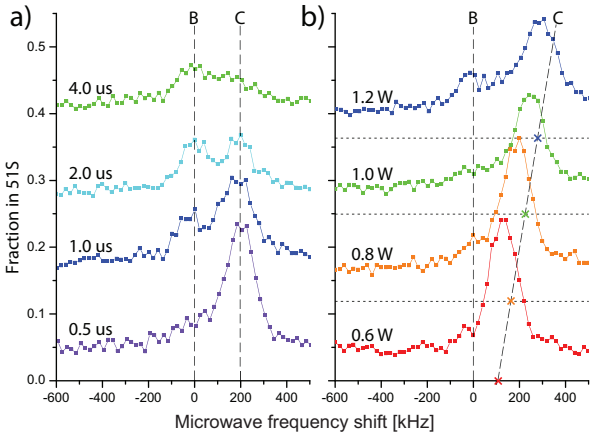

FIG. 4. (Color online.) Effect of varying excitation pulse length $\tau_{\rm ex}$ and lattice power P on trapping efficiency for $\eta = 1$ (complete lattice inversion). a) Varying $\tau_{\rm ex}$ at fixed P = 0.8 W. b) Varying P at fixed $\tau_{\rm ex} = 0.5$ μs.

$T = 100$ μK (used in Fig. 3), with respective estimated uncertainties of 2 μm and 20 μK. For these parameters, we find that 90% of the atoms are trapped in the fully inverted lattice ($\eta = 1$). We have studied how sensitive this result is to these parameters. Over a temperature range of 40 μK to 300 μK, the trapping efficiency decreases approximately linearly from 99% to 64%, with all other parameters unchanged. Variation of $w_{\rm r}$ from 13 μm to 40 μm leads to a linear drop of the trapping fraction from 95% to 84%. Hence, the temperature T affects the Rydberg-atom trapping efficiency the most. We believe that $w_{\rm r}$ is larger than the FWHM diameter of the incident beam because of cumulative aberrations caused by the optical components in the retro-reflection beam path (see Fig. 1).

Experimental microwave spectra for selected values of $\tau_{\rm ex}$ and $\eta = 1$ are shown in Fig. 4(a). As $\tau_{\rm ex}$ is increased, the C-signal in the microwave spectra diminishes while the B-signal grows. Lower values of $\tau_{\rm ex}$ therefore result in higher trapping efficiencies. This is because Rydberg atoms are excited at random times during the excitation pulse; however, the lattice is not inverted until the completion of the excitation pulse. For shorter $\tau_{\rm ex}$, the Rydberg atoms have, on average, less time to slide down the lattice potential wells before the lattice is inverted. The atoms then gain less kinetic energy, resulting in better trapping.

In Fig. 4(b), we show microwave spectra for several values of P. The detuning of the C-peaks scales linearly with trap laser power, as expected. For the three lowest powers, the spectral signal is almost entirely in the C-component, indicating efficient Rydberg-atom trapping. For the highest power of 1.2 W, the emerging B-signal indicates a loss in trapping efficiency. Simulations anal-

ogous to the ones in Fig. 3 show that this loss is in part due to a temperature increase of the optically trapped ground-state atoms to about 160 μK. We attribute the temperature increase to a deterioration of laser cooling, as the red-detuning of the MOT cooling light approaches ten linewidths in the lattice potential wells. Also, as P is increased, the excited atoms (partially) slide down steeper lattice potential wells before lattice inversion. Therefore, the kinetic energy that the atoms gain between optical excitation and lattice inversion increases with P. The simulations show that this effect is noticeable even at $\tau_{ex} = 0.5$ μs. As a result of both effects, the kinetic energy of the Rydberg atoms is higher in deeper lattices, leading to reduced Rydberg-atom trapping efficiency.

To study lattice-induced photo-ionization (PI), which could be a concern in applications, we have measured the Rydberg atom number as a function of delay time between excitation and detection. For 50S Rydberg atoms, measurements with and without optical lattice show exponential decays with identical lifetimes of 100±15 μs. Hence, there is no PI and the decay is entirely due to natural decay and decay induced by black-body radiation. The measured decay times are in line with anticipated values [15]. The absence of measurable PI reflects the low PI cross section of S Rydberg levels of Rb. Reference [16] shows a PI cross section of about 45 barns for the 50S state, while we have calculated 65 barns. Under our conditions, these cross sections translate into PI rates $< 100\,\mathrm{s}^{-1}$, which are too small to be detectable. For comparison, we have studied the decay of $50D_{5/2}$ Rydberg atoms, for which both Ref. [16] and our calculations show a PI cross section of about 1.3×10^4 barns. Here, we observe clear evidence of PI. Figure 5 demonstrates that $50D_{5/2}$ atoms in the lattice decay considerably faster than atoms without lattice. Also, PI occurs faster without lattice inversion ($\eta = 0$) than with inversion ($\eta = 1$). The latter observation is readily explained by the fact that the lattice inversion places the atoms at a lattice intensity minimum immediately after excitation, where the PI rate is lower.

To estimate the typical trapping time of Rydberg atoms in the lattice, we measure the ratio $F(t)$ of the Rydberg atom number with the lattice on divided by the number with the lattice off for the $50D_{5/2}$ state. $F(t)$ drops from an initial value of 1.0 to asymptotic values that are reached when all Rydberg atoms have either photo-ionized or have moved out of the lattice. Hence, $F(t)$ allows us to estimate the Rydberg atom dwell time in the lattice. Inspecting Fig. 5(c), we estimate dwell times of about 15 μs for $\eta = 0$ and somewhat larger values for $\eta = 1$. In the inverted case, the dwell time is expected to be longer because the PI rate is lower and because the atoms leave the lattice more slowly, as there is a smaller transverse gradient force pushing them out of the lattice.

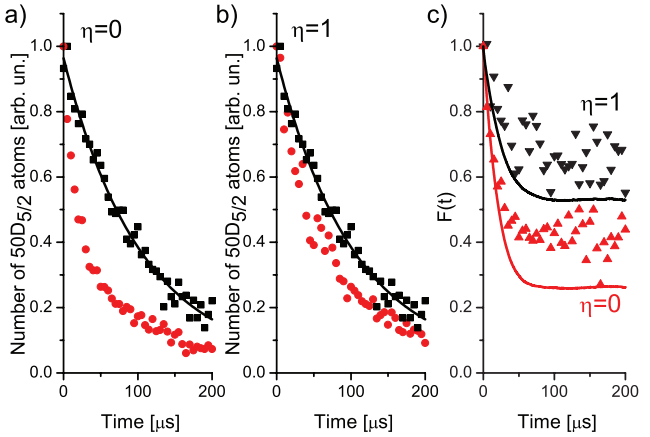

FIG. 5. (Color online.) Measurements of lattice-induced photo-ionization of $50D_{5/2}$ Rydberg atoms in an optical lattice ($P = 0.8$ W). Atom number vs time after excitation without (black squares) and with lattice (red circles) for $\eta = 0$ (a) and $\eta = 1$ (b). The data without lattice are fitted with an exponential function (lifetime 100±15 μs). c) Symbols: ratios $F(t)$ obtained from the experimental data in panels (a) and (b). Lines: simulation results.

Using the known trapping potentials [10], PI cross sections, and lattice-free decay rates, we have simulated the lattice-induced dynamics of 50S and $50D_{5/2}$ Rydberg atoms over 200 μs, taking decay processes into account. We find that the 50S and $50D_{5/2}$ atoms exhibit similar dwell times of several tens of μs in the lattice. As seen in the experiment, the $50D_{5/2}$ atoms undergo some PI-induced decay while they move out of the lattice. PI is insignificant for the 50S atoms. Simulated curves $F(t)$, included in Fig. 5(c), qualitatively agree with the experimental results. We attribute the deviations at late times to unaccounted-for reduction in PI cross section, which occurs when atoms transition from $50D_{5/2}$ into neighboring P- or F-states (mainly due to black-body radiation).

We have shown that a lattice inversion technique enables Rydberg-atom trapping in a red-detuned optical lattice with 90% efficiency. The trapping efficiency is expected to approach 100% after reduction of the initial atom temperature. Current work focuses on the attainment of three-dimensional trapping and long Rydberg atom dwell times in the lattice by the addition of axial confinement. We can expect a trapping time identical to the Rydberg-atom decay time (≈ 100 μs for 50S), which would be long enough for a sequence of gate operations in quantum information applications or for high-precision spectroscopy applications.

S.E.A. acknowledges fellowship support from DOE SCGF. This work was supported by NSF Grants No. PHY-0855871 and No. PHY-0114336.

*andsare@umich.edu

[1] D. Jaksch, J. I. Cirac, P. Zoller, S. L. Rolston, R. Côté, and M. D. Lukin, Phys. Rev. Lett. **85**, 2208 (2000).

[2] E. Urban *et al.*, Nature Phys. **5**, 110 (2009).

[3] A. Gaëtan *et al.*, Nature Phys. **5**, 115 (2009).

[4] M. Saffman, T. G. Walker and K. Mølmer, Rev. Mod. Phys. **82**, 2313 (2010).

[5] B. Knuffman and G. Raithel, Phys. Rev. A **75**, 053401 (2007).

[6] J. H. Choi, J. R. Guest, A. P. Povilus, E. Hansis, and G. Raithel, Phys. Rev. Lett. **95**, 243001 (2005).

[7] S. D. Hogan and F. Merkt, Phys. Rev. Lett. **100**, 043001 (2008).

[8] S. K. Dutta, J. R. Guest, D. Feldbaum, A. Walz-Flannigan, and G. Raithel, Phys. Rev. Lett. **85**, 5551 (2000).

[9] S. H. Friedrich, *Theoretical Atomic Physics* (Springer, Berlin, 2004).

[10] K. C. Younge, S. E. Anderson, and G. Raithel, New J. Phys. **12**, 023031 (2010).

[11] M. Marinescu, H. R. Sadeghpour, and A. Dalgarno, Phys. Rev. A **49**, 5103 (1994).

[12] K. C. Younge, B. Knuffman, S. E. Anderson, and G. Raithel, Phys. Rev. Lett. **104**, 173001 (2010).

[13] T. F. Gallagher, *Rydberg Atoms* (Cambridge University Press, Cambridge, U.K., 1994).

[14] K. C. Younge, S. E. Anderson, and G. Raithel, New J. Phys. **12**, 113036 (2010).

[15] I. I. Beterov, I. I. Ryabtsev, D. B. Tretyakov, and V. M. Entin, Phys. Rev. A **79**, 052504 (2009).

[16] M. Saffman and T. G. Walker, Phys. Rev. A **72**, 022347 (2005).